Modulational Instability and Parametric Amplification Induced by Loss Dispersion in Optical Fibers

Takuo Tanemura,* Yasuyuki Ozeki, and Kazuro Kikuchi

Research Center for Advanced Science and Technology, University of Tokyo, 4-6-1 Komaba, Meguro-Ku, Tokyo 153-8904, Japan

(Received 14 April 2004; published 13 October 2004)

We show that modulational instability may arise even in the normal group-velocity dispersion regime of an optical fiber when the fiber loss (gain) varies depending on the wavelength. A simple analytical expression for the instability gain is obtained, which reveals that the odd-order terms of the loss dispersion are responsible for this phenomenon. The instability gain is measured experimentally in an optical-parametric-amplification configuration. Large parametric gain is induced in a non-phase-matched regime as we apply narrow band loss at the idler wavelength.

DOI: 10.1103/PhysRevLett.93.163902 PACS numbers: 42.65.Sf, 42.65.Hw, 42.65.Yj, 42.81.Dp

Modulational instability (MI) is a general feature of wave propagation in dispersive nonlinear media and is exhibited in such diverse fields as fluid dynamics [1], plasmas [2], and nonlinear optics [3–5]. In particular, MI has been widely studied in the context of optical fibers [4,5], which provide pure one-dimensional and fairly stable environments for the observation of nonlinear optics. When a strong continuous-wave (cw) light propagates inside an optical fiber with weak perturbations, amplitude-modulational (AM) perturbation converts to the phase-modulational (PM) perturbation through the optical Kerr effect, while the PM perturbation is transferred back to the AM perturbation by the group-velocity dispersion (GVD). In the anomalous GVD regime, these effects provide positive feedback, resulting in MI, i.e., the exponential growth of the perturbations. MI can be explained alternatively as the process of optical-parametric amplification (OPA), where the anomalous GVD is required to satisfy the phase-matching condition among the pump carrier and two modulational sidebands [5]. In this context, observation of MI in the normal-GVD regime has been limited to special cases in which an extra phase shift is provided by an additional copropagating pump mode [6–11], by the higher-order GVD [12], or in a ring cavity configuration [13,14].

In this Letter, we show that a novel type of MI occurs in the normal-GVD regime when the fiber loss varies depending on the wavelength. Unlike the standard scalar MI in the anomalous GVD regime, the PM-to-AM conversion of the pump perturbation is induced by the loss dispersion instead of GVD. Assuming general profiles of both the loss (or gain) and GVD, we obtain a simple analytical expression for the MI gain, which indicates the explicit conditions for inducing MI in the normal-GVD regime. We then demonstrate direct observation of the loss-induced MI in an OPA configuration. Significant enhancement of the OPA gain is observed in a non-phase-matched regime of a fiber as we induce narrow band distributed loss at the idler wavelength.

In fact, the closely related phenomenon of Raman-assisted OPA has been discovered by several authors [15,16], in which the Raman resonance is proved to enhance the OPA gain in a non-phase-matched regime. In addition, the recent analytical work on MI in a rare-earth-doped fiber amplifier claims that MI occurs in the normal-GVD regime when the pump is placed at the slope of the gain spectrum [17]. Our analysis reveals that the wavelength-dependent gain, induced by either Raman effect or rare-earth doping, is not necessarily required but any odd-order (asymmetrical) loss dispersion in general may cause MI in the normal-GVD regime.

In the linearized regime of MI, or equivalently, under the undepleted-pump approximation of OPA, wave evolution along the fiber is described by the coupled-mode equations [5]:

$$\frac{dA_0}{dz} = i\gamma|A_0|^2A_0 - \frac{1}{2}\alpha_0 A_0, \tag{1}$$

$$\frac{dA_+}{dz} = i\gamma(2|A_0|^2A_+ + A_0^2A_-^*e^{-i\Delta kz}) - \frac{1}{2}\alpha_+ A_+, \tag{2}$$

$$\frac{dA_-}{dz} = i\gamma(2|A_0|^2A_- + A_0^2A_+^*e^{-i\Delta kz}) - \frac{1}{2}\alpha_- A_-, \tag{3}$$

where A_0 is the slowly varying envelope of the pump carrier, whereas A_+ and A_- are those of the upper and lower sidebands of the weak modulation, respectively. $\gamma = 2\pi n_2/(\lambda A_{\text{eff}})$ (n_2 is the nonlinear refractive index, λ is the wavelength, and A_{eff} is the effective core area of the fiber) is the nonlinear coefficient and $\Delta k \equiv k_+ + k_- - 2k_0$ (k_j are the propagation constants of respective waves) denotes the linear phase mismatch. The wavelength dependence of γ is ignored in the case of our interest. The additional terms $\alpha_j A_j/2$ represent the absorption ($\alpha_j > 0$) or gain ($\alpha_j < 0$) experienced by respective waves. We assume $\alpha_+ \geq \alpha_-$ for simplicity.

From Eq. (1), A_0 is solved as $A_0(z) = \sqrt{P_0}\exp[i\int_0^z \times \gamma P(z')dz' - \alpha_0 z/2]$, where $P(z) = P_0\exp(-\alpha_0 z)$ is the local pump power. By introducing new variables

$\psi_{AM} = B_+ + B_-^*$ and $\psi_{PM} = -i(B_+ - B_-^*)$, where $B_\pm = A_\pm \exp[-i\int_0^z \gamma P(z')dz' + \alpha_0 z/2 + i\Delta k z/2]$, Eqs. (2) and (3) yield

$$\frac{d\psi_{AM}}{dz} = -\frac{1}{4}(\alpha_+ + \alpha_- - 2\alpha_0)\psi_{AM} - \frac{1}{2}\Delta k\psi_{PM} - \frac{i}{4}(\alpha_+ - \alpha_-)\psi_{PM}, \quad (4)$$

$$\frac{d\psi_{PM}}{dz} = -\frac{1}{4}(\alpha_+ + \alpha_- - 2\alpha_0)\psi_{PM} + \frac{1}{2}\Delta k\psi_{AM} + \frac{i}{4}(\alpha_+ - \alpha_-)\psi_{AM} + 2\gamma P(z)\psi_{AM}. \quad (5)$$

Physically, ψ_{AM} and ψ_{PM} represent the AM and PM components of the perturbation, respectively. Equations (4) and (5) clearly reveal that the coupling between the AM and PM perturbations occurs not only through the GVD term $\Delta k/2$, but also through the loss-dispersion term $i(\alpha_+ - \alpha_-)/4$.

Under the lowest-order approximation of Wentzel-Kramers-Brillouin expansion (valid when $\gamma P \gg \alpha_0$) [18], the solution to Eqs. (4) and (5) can be written as $\psi_{AM,PM} \equiv \psi_{AM0,PM0}\exp[\int_0^z \gamma P(z')\kappa(z')dz']$. As a result, we obtain the eigenvalue equation

$$\begin{pmatrix} -\alpha_{even} & -d - i\alpha_{odd} \\ (d+2) + i\alpha_{odd} & -\alpha_{even} \end{pmatrix}\begin{pmatrix} \psi_{AM0} \\ \psi_{PM0} \end{pmatrix} = \kappa\begin{pmatrix} \psi_{AM0} \\ \psi_{PM0} \end{pmatrix}, \quad (6)$$

where we introduce $d(z) = (k_+ + k_- - 2k_0)/2\gamma P$, $\alpha_{odd}(z) = (\alpha_+ - \alpha_-)/4\gamma P$, and $\alpha_{even}(z) = (\alpha_+ + \alpha_- - 2\alpha_0)/4\gamma P$. The normalized phase mismatch factor d is proportional to the even-order GVD at the pump wavelength, whereas α_{odd} and α_{even} are the normalized odd- and even-order terms of the loss dispersion, respectively. The eigenvalue κ of Eq. (6) is solved as

$$\kappa = -\alpha_{even} \pm (g + i\phi), \quad (7)$$

where

$$g \equiv \mathrm{Re}\sqrt{\alpha_{odd}^2 - d(d+2) - i2\alpha_{odd}(d+1)} = \frac{1}{\sqrt{2}}\sqrt{\alpha_{odd}^2 - d(d+2) + \sqrt{\alpha_{odd}^4 + 2\alpha_{odd}^2(d^2+2d+2) + d^2(d+2)^2}}, \quad (8)$$

$$\phi \equiv \mathrm{Im}\sqrt{\alpha_{odd}^2 - d(d+2) - i2\alpha_{odd}(d+1)} = -\frac{\mathrm{sgn}(d+1)}{\sqrt{2}}\sqrt{-\alpha_{odd}^2 + d(d+2) + \sqrt{\alpha_{odd}^4 + 2\alpha_{odd}^2(d^2+2d+2) + d^2(d+2)^2}}. \quad (9)$$

Finally, we obtain an analytical expression for the local power gain $G(z)$ of the two sidebands:

$$G = -\alpha_0 + 2\gamma P\mathrm{Re}(\kappa) = -\alpha_- + 2\gamma P f_-, \quad (10)$$

where $f_- = g - \alpha_{odd}$. Since $G = -\alpha_-$ for the lower sideband in the absence of nonlinearity, $2\gamma P f_-$ represents the additional MI gain experienced by the lower sideband. Note that f_- is determined uniquely by two normalized parameters, d and α_{odd}, which are responsible for the PM-to-AM conversion of the perturbation in Eq. (6).

Figure 1(a) shows the contour plot of f_- calculated as a function of d and α_{odd}. The solid lines are the contour lines on which $f_- = 0.1, 0.2$, etc., while the dotted lines indicate minor contour lines with every 0.02 interval. When $\alpha_{odd} = 0$, f_- is nonzero only within the range of $-2 < d < 0$ and takes the maximum value of 1 at $(d, \alpha_{odd}) = (-1, 0)$. This corresponds to the standard scalar MI in the anomalous GVD regime [4,5]. The noteworthy feature in Fig. 1(a) is that when $\alpha_{odd} > 0$, f_- becomes positive for an arbitrary value of d, even in the normal-GVD regime ($d > 0$). This clearly indicates the existence of a novel type of MI induced by the odd-order loss dispersion.

By solving the eigenmode (ψ_{AM0}, ψ_{PM0}) in Eq. (6), we also calculate the sideband power ratio $|A_-|^2/|A_+|^2$ of the MI eigenmode:

$$\frac{|A_-|^2}{|A_+|^2} = \frac{(\phi - d)^2 + (g + \alpha_{odd})^2}{(\phi + d)^2 + (g - \alpha_{odd})^2}. \quad (11)$$

Figure 1(b) shows $|A_-|^2/|A_+|^2$ on the (d, α_{odd}) plane. While $|A_+|^2 = |A_-|^2$ in the usual MI regime ($-2 < d < 0$, $\alpha_{odd} = 0$), $|A_-|^2/|A_+|^2$ increases with α_{odd}, implying that the lower sideband grows dominantly for large α_{odd}. Such MI is similar to the single-sideband MI, which emerges in the two-pump configuration [11]. This is also consistent with the recent Letter on the Raman-assisted OPA [16], where it is explained that the power imbalance between two sidebands leads to the self-induced phase matching.

The loss-induced MI gain is measured experimentally in an OPA configuration; a small signal light is seeded at the fiber input, which acts as an initial modulational perturbation to the strong pump carrier. As a simple example of odd-order loss- dispersion, large distributed loss α_i is induced at the idler wavelength as illustrated in the inset of Fig. 2. Although the pump wave is placed in the normal-GVD regime, we expect the signal wave to grow exponentially by experiencing the loss-induced MI gain as we increase α_i. To realize the wavelength-selective loss experimentally, we exploit stimulated Brillouin scattering (SBS) inside the fiber. By injecting a strong SBS pump light from the opposite end of the fiber and redshifting its wavelength exactly by the Brillouin

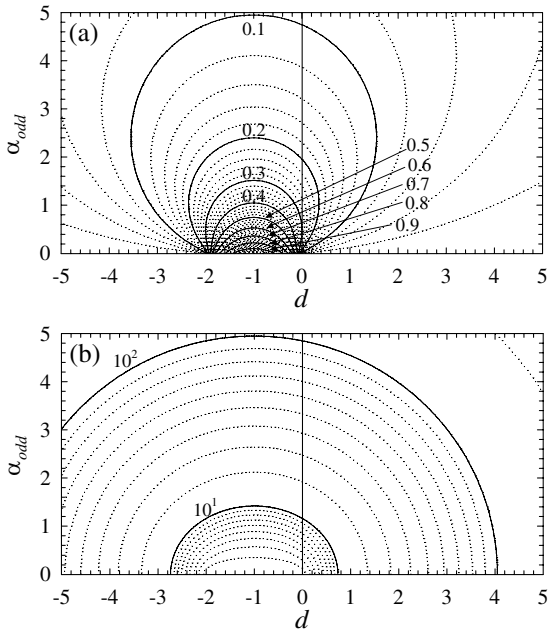

FIG. 1. (a) Contour plot of the normalized MI gain for the lower sideband f_- calculated as a function of d and α_{odd}. When $\alpha_{\text{odd}} = 0$, f_- is nonzero only in the anomalous GVD regime ($-2 < d < 0$). However, f_- becomes positive in the normal-GVD regime ($d > 0$) when $\alpha_{\text{odd}} > 0$. (b) Contour plot (in log scale) of the power ratio between two sidebands $|A_-|^2/|A_+|^2$ as a function of d and α_{odd}. While $|A_+|^2 = |A_-|^2$ in the usual MI regime ($-2 < d < 0$, $\alpha_{\text{odd}} = 0$), $|A_-|^2/|A_+|^2$ increases with α_{odd}, implying that the lower sideband grows dominantly for large α_{odd}.

frequency from the idler wave, we induce narrow band anti-Stokes absorption at the idler wavelength [19].

The experimental setup is shown in Fig. 2. Two external-cavity semiconductor lasers, ECL1 and ECL2, generated the OPA pump and signal waves at 1542.0 and 1543.8 nm, respectively. After combined by a 1:9 directional coupler, they were modulated with square-pulse trains using an electroabsorptive modulator (EAM). The modulated pulses could be assumed quasi-cw with the pulse duration of 4.7 ns and the repetition rate of 1.7 MHz. They were then amplified by an erbium-doped fiber amplifier (EDFA) and launched on a 1-km-long highly nonlinear dispersion-shifted fiber (HNL-DSF), which had the propagation loss of 1.1 dB/km, zero-dispersion wavelength at 1554 nm, and dispersion slope of 0.028 ps/km/nm^2. The Brillouin frequency of HNL-DSF was 9.35 GHz, which was measured by injecting a strong cw light and observing the beat spectrum between the cw and scattered Stokes waves. The nonlinear coefficient γ was measured to be 19.5 km^{-1} W^{-1} by the four-wave mixing method [20]. The peak powers of the OPA pump and signal pulses were estimated to be 1.05 W and 0.34 mW at the input of HNL-DSF, respectively. Note that the pump wave was located in the normal-GVD regime (-0.34 ps/km/nm, $d = 0.02$), so that the standard scalar MI was strictly inhibited.

We then injected the SBS pump from the opposite end of HNL-DSF. It was phase modulated with a specially coded binary pattern at 2 Gbit/s [19], which broadened the absorption spectrum uniformly over 2 GHz, covering the entire idler bandwidth (<1 GHz). Finally, we monitored the beat spectrum between the SBS pump and generated idler wave and tuned the wavelength of the SBS pump accordingly, so that the frequency difference is maintained to the Brillouin frequency (9.35 GHz) within $\pm$20-MHz accuracy. By adjusting the incident power of the SBS pump, we could control the idler loss as shown in Fig. 3(a). The output signal power was measured using a high-resolution optical spectrum analyzer.

One problem of the SBS-induced loss is that it inevitably induces a phase shift to the idler wave whenever the absorption peak deviates slightly from the idler wavelength [19]. Therefore, although we may observe the OPA gain increase when injecting the SBS pump, it is quite ambiguous whether it is caused by the loss itself or by the SBS-induced phase shift, which changes Δk. To avoid this problem, we have selected the signal wavelength as follows. First, we turned off the SBS pump and measured the output signal power as a function of signal wavelength. Then, from the obtained OPA gain spectrum, plotted in Fig. 3(b), we decided the signal wavelength to be at 1543.8 nm, the first peak of the gain spectrum. In such a case, the gain is relatively insensitive to Δk, and more-

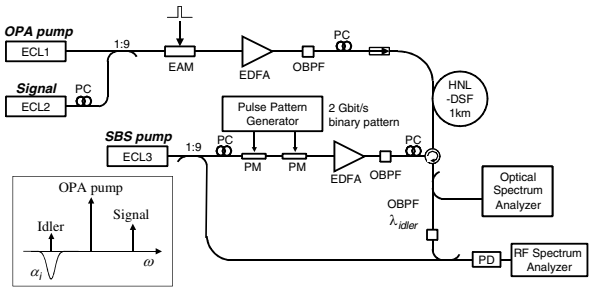

FIG. 2. Experimental setup for observing the loss-induced MI in an OPA configuration. PC: polarization controller, OBPF: optical bandpass filter, PM: $LiNbO_3$ phase modulator, PD: photodetector.

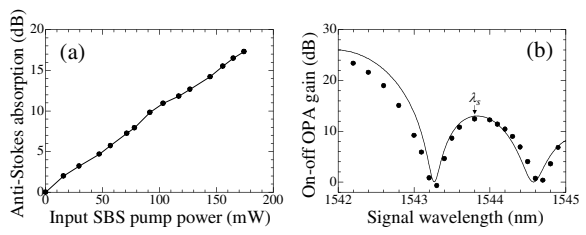

FIG. 3. (a) SBS-induced absorption at the idler wavelength measured as a function of input SBS pump power. (b) Measured (dots) and theoretical (solid line) OPA gain spectrum without injecting the SBS pump. The signal wavelength was chosen at the first peak of the spectrum, so that any SBS-induced phase shift would only degrade the OPA gain.

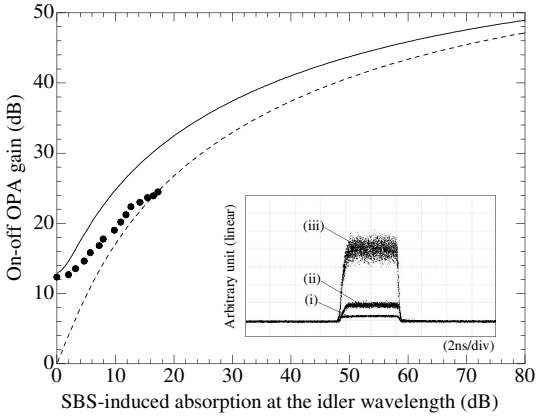

FIG. 4. On-off signal gain (dots) measured as a function of the idler loss. Solid and broken curves indicate the theoretical OPA gain and the MI gain, respectively. The inset shows the output signal waveforms observed when the idler loss was (i) 0 dB, (ii) 7.9 dB, and (iii) 17.3 dB.

over, a small change in Δk would only degrade the gain. Therefore, any gain enhancement observed when injecting the SBS pump could be attributed clearly to the SBS-induced loss.

Figure 4 shows the on-off OPA gain measured as a function of the SBS-induced loss at the idler wavelength. The on-off OPA gain is defined as the output signal power when the OPA pump is turned on, relative to that without the OPA pump. Output signal waveforms are also shown in the inset for three different values of idler loss: (i) 0 dB, (ii) 7.9 dB, and (iii) 17.3 dB. We can see that the OPA gain is enhanced by more than 10 dB when we apply 17.3-dB absorption at the idler wavelength. The broken curve shows the theoretical MI gain, $\exp(Gz) = \exp(2\gamma P f_{-} z)$ [Eq. (10)], whereas the solid curve is the OPA gain $|A_{-}(z)|^2/|A_{-}(0)|^2$ calculated analytically from Eqs. (1)–(3) with $\alpha_0 = \alpha_{-} = 0$, $\alpha_{+} = \alpha_i$, and the boundary condition of $A_{+}(0) = 0$. Note that the OPA gain converges to the MI gain at large idler loss. Although no fitting parameter was used in the calculation, we can see reasonable agreement between the measured and calculated gains in Fig. 4. The quantitative differences should be attributed to the background fiber loss, polarization mode dispersion, longitudinal fluctuation of the zero-dispersion wavelength, etc., which are all ignored in the calculation.

In conclusion, we have found a novel type of MI that arises in the normal-GVD regime of an optical fiber with wavelength-dependent loss. Assuming general profiles of GVD and loss dispersion, we obtained a simple analytical expression for the MI gain, which reveals that the odd-order loss dispersion is responsible for such instability. The underlying physics is that the odd-order loss dispersion yields PM-to-AM conversion of the pump perturbation, which interacts with the Kerr-induced AM-to-PM conversion to provide positive feedback. Observation of the loss-induced MI gain was demonstrated in an OPA configuration. A large OPA gain was induced in a non-phase-matched regime of fiber as we applied narrow band distributed loss at the idler wavelength by using SBS. These results indicate an exciting possibility of extending the OPA bandwidth into the non-phase-matched regime by an elaborate design of both the loss and GVD profiles of the fiber. For example, unpumped rare-earth-doped fibers or long-period fiber Bragg gratings can be interesting candidates for realizing ultrabroadband OPA, which is highly desired in optical communication systems. Finally, we should note that although we have employed an optical fiber in the experiment, the analysis should be applicable to other nonlinear dispersive systems as well and may find novel application in different branches of physics.

*Electronic address: tanemura@ginjo.rcast.u-tokyo.ac.jp

[1] T. B. Benjamin and J. E. Feir, J. Fluid Mech. **27**, 417 (1967).
[2] T. Taniuti and H. Washimi, Phys. Rev. Lett. **21**, 209 (1968).
[3] L. A. Ostrovskii, Zh. Eksp. Teor. Fiz. **51**, 1189 (1966) [Sov. Phys. JETP **24** , 797 (1967)].
[4] K. Tai, A. Hasegawa, and A. Tomita, Phys. Rev. Lett. **56**, 135 (1986).
[5] G. P. Agrawal, *Nonlinear Fiber Optics* (Academic, New York, 2001), 3rd ed.
[6] A. L. Berkhoer and V. E. Zakharov, Zh. Eksp. Teor. Fiz. **58**, 903 (1970) [Sov. Phys. JETP **31**, 486 (1970)].
[7] P. D. Drummond, T. A. B. Kennedy, J. M. Dudley, R. Leonhardt, and J. D. Harvey, Opt. Commun. **78**, 137 (1990); J. E. Rothenberg, Phys. Rev. A **42**, 682 (1990).
[8] G. P. Agrawal, Phys. Rev. Lett. **59**, 880 (1987).
[9] G. Millot, S. Pitois, P. T. Dinda, and M. Haelterman, Opt. Lett. **22**, 1686 (1997).
[10] S. Wabnitz, Phys. Rev. A **38**, 2018 (1988).
[11] T. Tanemura and K. Kikuchi, J. Opt. Soc. Am. B **20**, 2502 (2003).
[12] J. D. Harvey, R. Leonhardt, S. Coen, G. K. L. Wong, J. C. Knight, W. J. Wadsworth, and P. St. J. Russell, Opt. Lett. **28**, 2225 (2003).
[13] M. Haelterman, S. Trillo, and S. Wabnitz, Opt. Lett. **17**, 745 (1992).
[14] S. Coen and M. Haelterman, Phys. Rev. Lett. **79**, 4139 (1997).
[15] T. Sylvestre, H. Maillotte, E. Lantz, and P. T. Dinda, Opt. Lett. **24**, 1561 (1999).
[16] S. Coen, D. A. Wardle, and J. D. Harvey, Phys. Rev. Lett. **89**, 273901 (2002).
[17] T. Mirtchev, J. Opt. Soc. Am. B **15**, 171 (1998).
[18] M. Karlsson, J. Opt. Soc. Am. B **12**, 2071 (1995).
[19] T. Tanemura, Y. Takushima, and K. Kikuchi, Opt. Lett. **27**, 1552 (2002).
[20] K. Kikuchi, K. Taira, and N. Sugimoto, Electron. Lett. **38**, 166 (2002).